[4] Strieff, M. L. and Ferriso, C. C., "Spectral Slit Width of a Small Prism Monochromator," GDA-DBE64-054, Aug. 1964, General Dynamics/Astronautics, Space Science Lab., San Diego, Calif.

[5] "JANAF Thermochemical Tables," The Dow Chemical Company, Midland, Mich.

[6] Wentink, T., "High Temperature Behavior of Teflon," Research Rept. 55, July 1959, Avco Everett Research Lab.

[7] Settlage, P. H. and Siegle, J. C., "Behavior of Teflon Fluorocarbon Resins at Elevated Temperatures," *Planetary and Space Science*, Vol. 3, 1961, pp. 73–81.

[8] Modica, A. P. and Sillers, S. J., "Experimental and Theoretical Kinetics of High-Temperature Fluorocarbon Chemistry," *The Journal of Chemical Physics*, Vol. 48, No. 7, April 1968, pp. 3283–3289.

[9] Gaydon, A. G., *The Spectroscopy of Flames*, Chapman and Hall, London, 1957, Chap. VIII.

[10] Kiess, N. H. and Broida, H. P., *Seventh Symposium on Combustion*, Butterworth, London, 1959, p. 207.

APRIL 1970 AIAA JOURNAL VOL. 8, NO. 4

Failure of Existing Theories to Correlate Experimental Nonacoustic Combustion Instability Data

T. L. Boggs*
Naval Weapons Center, China Lake, Calif.

AND

M. W. Beckstead†
Lockheed Propulsion Company, Redlands, Calif.

Experimental data concerning nonacoustic combustion instability of solid propellants are presented and compared with the predictions of theoretical models. This comparison reveals that the models are inadequate to predict the bulk mode instability behavior of certain propellants such as those using a polyurethane binder. A computational method, the layer frequency concept, is proposed. The results obtained using this technique suggest that the heterogeneity of the propellant and the relationship of the thermal wave thickness to the oxidizer particle sizes are factors that cannot be neglected (as they are in the theoretical models) in the modeling of nonacoustic combustion instability of a propellant system.

Nomenclature

A = nondimensional parameter in the response function (see Ref. 14)
B = nondimensional parameter in the response function (see Ref. 14)
D = oxidizer particle diameter
f = frequency of oscillations, cps
L^* = characteristic length of chamber (free volume divided by nozzle throat area)
$\overline{MW}$ = molecular weight of combustion chamber gases
n = pressure exponent in steady-state burning rate equation $\bar{r} = b\bar{p}^{-n}$
$\bar{p}$ = mean- or time-average pressure
p' = pressure perturbation
$Re\ (\ldots)$ = real part of a complex expression
R = response function $= (r'/\bar{r})/(p'/\bar{p})$
$\bar{r}$ = mean burning rate
r' = burning rate perturbation
T_f = adiabatic flame temperature
x = weight fraction of oxidizer
α = exponential growth rate
α_t = thermal diffusivity of solid
δ = characteristic binder thickness between oxidizer particles
λ = characteristic root of solid phase energy equation (see Eq. 3)
ρ_{ox} = oxidizer density
ρ_f = binder density
τ = characteristic time
τ_{ch} = residence time of the chamber $= c^*L^*\overline{MW}/RT_f$
τ_{tw} = thermal wave relaxation time $= \alpha_t/\bar{r}^2$
Ω = nondimensional frequency $= \alpha_t\omega/\bar{r}^2$
ω = frequency, rad/sec

Presented as Paper 69-175 at the AIAA 7th Aerospace Sciences Meeting, New York, January 20–22, 1969; submitted February 6, 1969, revision received September 8, 1969. This work was supported by NASA under NASA Work Order 6030.

* Research Engineer, Aerothermochemistry Division. Member AIAA.

† Technical Specialist, Engineering Research Department Associate Fellow AIAA.

Introduction

A NUMBER of studies[1–12] have discussed the subject of oscillatory behavior of solid-propellant combustion in low-frequency modes (low compared to acoustic wave modes). Relevant analytical studies[1–4,6] have included modeling of the behavior of the combustor flow system as well as modeling of the perturbation behavior of the propellant combustion. Modeling of the over-all combustion-flow system has been simplified by decoupling the combustor analysis from the combustion zone analysis, using the mass response function as a matching condition to join the two separate analyses.[5] This has permitted better identification of the relationship between nonacoustic instability (NAI) and acoustic instability, and has permitted the relatively well-developed one-dimensional perturbation theory of solid-propellant combustion to be incorporated into the stability analysis for the combustor. These advances permit a much more decisive correlation between theory and the voluminous results of laboratory tests using the L^*-burner[3,5,7,8,10,12] and also advance the possibility of determining whether the experimental results can be used to test the validity of theory. Recently some comparison of this type have been made, which question the validity of the one-dimensional combustion perturbation models.[9–13] The results of the present work with com-

posite propellants further highlight certain inadequacies of the theory.

Propellants and Test Conditions

Two series of propellants were formulated and fired in the present study. One series used a polyurethane (PU) binder (at 25% by weight); the other series used a carboxy-terminated polybutadiene (CTPB) binder (also at 25% by weight). Mixed with these binders were carefully screened 15-, 45-, 90-, 200-, 400-, and 600-μ diameter particles of special spherical AP (ammonium perchlorate) to produce the propellants described in Table 1.

It should be noted that within the two series, the propellants are chemically identical; the only difference between propellants A-148 and A-155, for example, is the size of the oxidizer particles. These propellants were cut into 0.25-in.-thick by 1.6-in.-diam disks and burned in the L^*-burner as described in Ref. 7. Use of this laboratory device allowed data to be obtained between pressures of 30 and 200 psia, and L^* values of 20 to 100 in. The quantities measured from the tests were the growth rate, α, of oscillations, and the frequency. The value of L^*, calculated from the burner geometry, was used to calculate τ_{ch},[5] and the response function was then calculated from Eq. (1).[5] It should be realized that the range of conditions under which oscillatory behavior will occur in an NAI burner is extremely limited.[13] The test data, therefore, fit only a limited part of the response function curve.

Results and Discussion

The results of two areas of analysis make it possible to compare experimental data with theory. Modeling of the dynamics of the combustor-flow system leads to

$$(r'/\bar{r})/(p'/\bar{p}) = R = 1 + \alpha\tau_{ch} + i\omega\tau_{ch} \qquad (1)$$

This equation shows that a given oscillatory situation in the combustor (as defined by values of ω, τ_{ch}, and α) is uniquely related to the response of the combustion zone.

The relationship of the response function to the combustion of the propellant (hence to propellant characteristics) has been developed analytically by one-dimensional modeling of the combustion zone response to pressure disturbances. These models yield an expression for the response function in the form[14]

$$R = n\,AB/[\lambda + A/\lambda - (1 + A) + AB] \qquad (2)$$

where λ is the complex solution to the equation

$$\lambda(\lambda - 1) = i\,\alpha_t\omega/\bar{r}^2 = i\Omega \qquad (3)$$

Table 1 Propellant formulations

Propellant designation	Ingredients and weight percent					
	Ammonium perchlorate				Binder,	Carbon black,
	%	μ	%	μ	%	%
					(Polyurethane)	
A-146	37.5	15	37.5	80	25	...
A-148	37.0	15	37.0	200	25	1
A-149	37.0	90	37.0	600	25	1
A-151	37.0	45	37.0	200	25	1
A-155	37.0	45	37.0	400	25	1
A-156	51.8	15	22.2	200	25	1
A-157	22.2	15	51.8	200	25	1
					(CTPB)	
A-167	37.0	15	37.0	80	25	1
A-168	37.0	15	37.0	200	25	1
A-169	37.0	90	37.0	600	25	1
A-170	37.0	45	37.0	200	25	1
A-171	37.0	45	37.0	400	25	1
A-172	51.8	15	22.2	200	25	1

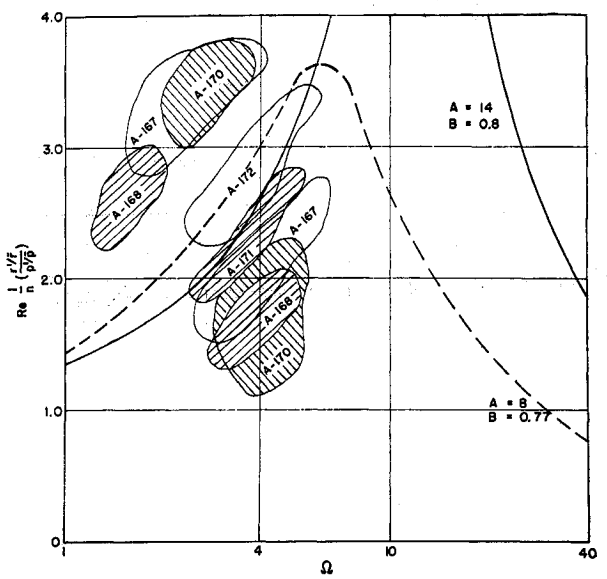

Fig. 1 Response function vs nondimensional frequency for CTPB-ammonium perchlorate propellants.

The parameter A is characteristic of the solid phase, while the parameter B depends principally on properties of the gas phase (see Ref. 14 for a summary of the various definitions of B). A common conclusion of the many models is that at the low frequencies of nonacoustic instability, the response of the solid phase is the dominant factor in determining the character of the instability. This indicates that the burning rate of the propellant should be a more general correlating parameter than the pressure (although Refs. 1, 2, and 4 use pressure as the correlating parameter). The effect of mean chamber pressure, therefore, has been found in these theories to be representable in terms of the pressure exponent, n, and the burning rate, r, with the rate dependence accommodated by use of the normalized frequency variable, Ω. According to Eq. (2) the response function (real part) of a given propellant should thus be insensitive to mean pressure when plotted against Ω, except as the steady-state pressure exponent, n, or the parameters, A and B, may be pressure dependent. Thus one might expect a graph of experimentally determined values of $Re\ R/n$ vs Ω to yield a single curve independent of pressure, and experimental results have been reported in the past in a format motivated by that expectation.

Employing Eq. (1) and plotting the data for the CTPB propellants as $Re\ /Rn$ vs Ω (Fig. 1), a correlation between theory and experimental data can be made; with one class of exceptions. These exceptions (certain high values of $Re\ R/n$ were caused by plateaus in the burning rate curve, which caused the value of n to approach zero, thus giving the larger values of the response function. On the other hand, the data for the polyurethane propellants, when plotted in the same manner, did not exhibit the trend of the theoretical curves (Fig. 2).

In comparing experimentally determined response function data with theory, it was necessary to estimate values of the propellant parameters, A and B, as was done for Figs. 1 and 2. Lacking any independent determination of these parameters, values can be adjusted to obtain the best fit between experiment and theory (although for the data shown in Fig. 2 no values of the parameters could give a reasonable fit). This arbitrariness obviously leaves open the possibility of agreement between theory and experiment even if the theory is wrong. However, there are some bounds to the present ignorance of which values of A and B are to be used—for example, A as normally defined,[14] is proportional to an activation energy and therefore must be positive. However, if it becomes necessary to use completely implausible values

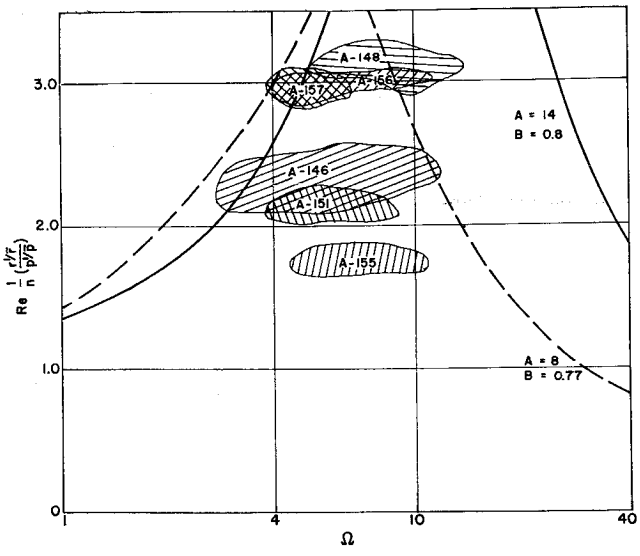

Fig. 2 Response function vs nondimensional frequency for polyurethane-ammonium perchlorate propellants.

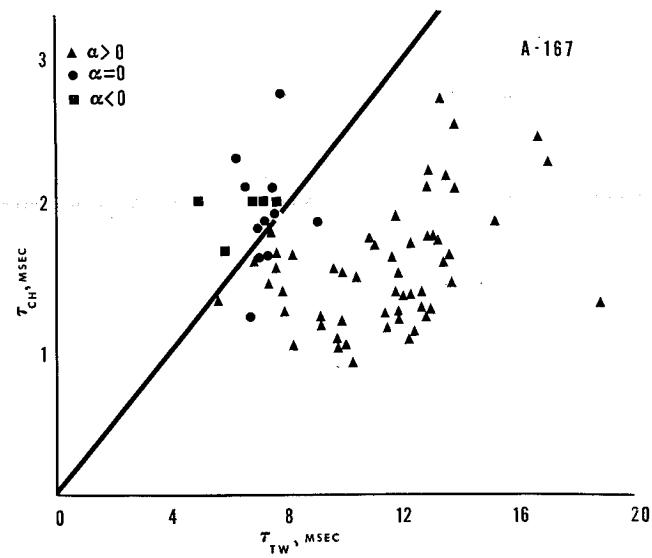

Fig. 4 Stability plot of τ_{ch} vs τ_{tw}, showing the stability limits ($\alpha = 0$) for CTPB propellants.

of A and B to fit the analysis to experimental results, then the analysis becomes suspect. This point is particularly well tested by plotting the experimental results in an $\omega\tau_{ch}$ vs Ω diagram. It is shown in Ref. 9 that for a given value of n, the $\omega\tau_{ch} - \Omega$ plane can be mapped from the theory with a family of curves of constant A and a family of curves of constant B. Plotting experimental values of $\omega\tau_{ch} - \Omega$ will give an estimate of the values of A and B required to fit the data to the theories discussed previously (see Fig. 3). Not only does an $\omega\tau_{ch}$ vs Ω diagram give a quick check on effective values of A and B, it may in the process provide a test of the credibility of the theory by the values of A and B dictated by the data. In particular, there is a region of the $\omega\tau_{ch} - \Omega$ plane in which solutions exist only for negative values of A. As can be seen in Fig. 3, some experimental data fall into this region,[9] indicating a failure of the analytical model to relate even the qualitative aspects of the actual combustion behavior.

The plot of $\omega\tau_{ch}$ vs Ω also indicates that behavior of the polyurethane propellants is not amenable to theoretical prediction, while that of the CTPB propellants is amenable to these predictions to a certain extent. This may be seen in Fig. 3 where the CTPB propellants usually give realistic values of A and B, while the data for several of the polyurethane propellants require values of A less than zero (which is physically impossible).

When the data are plotted as τ_{ch} vs τ_{tw}, the data having $\alpha > 0$ should be to the right of the stability limit[8]; the $\alpha = 0$ points should be on the line; and the $\alpha < 0$ data should be to the left of the line (in the stable domain). Theoretically, this line should pass through the origin with the slope depending on the values of A, B, and n.[8] The stability lines for the CTPB propellants (a typical plot is shown in Fig. 4) indeed pass through the origin, again indicating qualitative agreement with theory.

As in Figs. 2 and 3, also in the case of $\tau_{ch} - \tau_{tw}$ diagram, the data for the polyurethane propellants are not in agreement with theory. Figure 5 shows the data for propellant A-155 plotted as τ_{ch} vs τ_{tw}, and all of the other polyurethane propellants tested displayed similar anomalies. Here, all the data having $\alpha > 0$ are to the right of the line which intersects the abscissa at $\tau_{tw} = 20$ msec. The data to the left of this line were obtained for very low frequencies; frequencies much lower than theoretically predicted for the given conditions.

Thus, when the data are plotted in the manner suggested by the models, it can be seen that the models are inadequate to predict the instability characteristics of the polyurethane propellants. These same models are able to correlate the

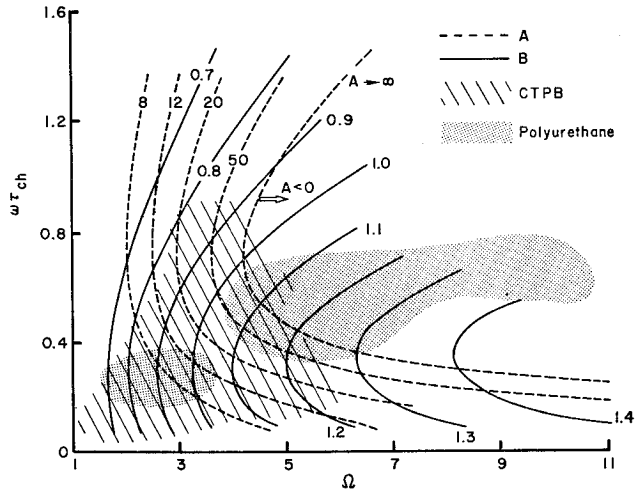

Fig. 3 L^*-chart for determining the parameters A and B, for the case, $n = 0.5$ (see Ref. 9).

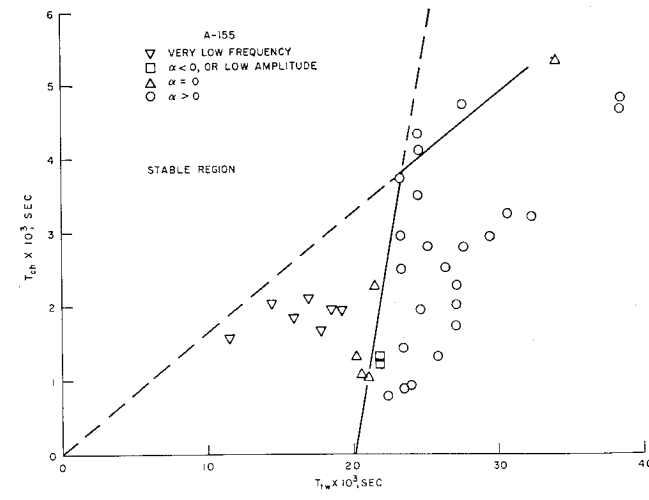

Fig. 5 Stability plot of τ_{ch} vs τ_{tw} for propellant A-155.

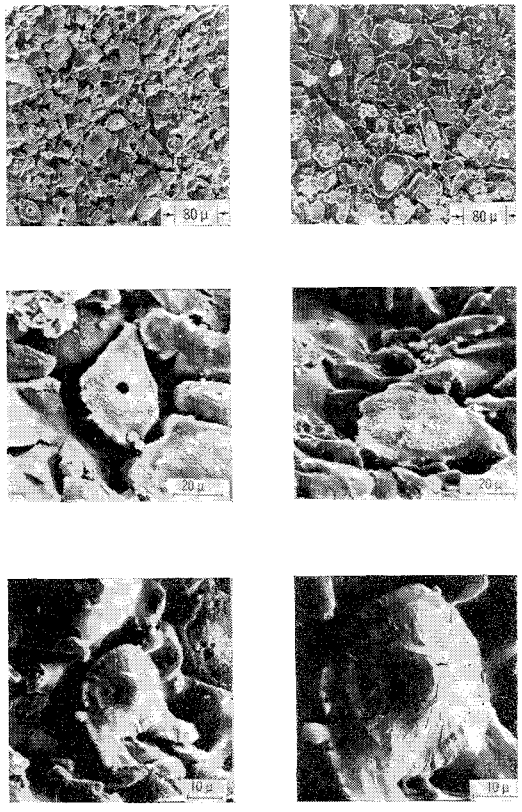

Fig. 6 Scanning electron microscope micrographs of a polyurethane-ammonium perchlorate propellant which had been burning at 200 psia.

CTPB data to a limited extent but only in a qualitative fashion.

In an effort to understand why these models are able to correlate the data for some propellants and not for others, the basis of the models was examined. Assumptions are involved in all of the models to make the description of the combustion mathematically tractable. Some of the most commonly used assumptions include: 1) a laminar, one-dimensional flame standing off from the propellant surface, 2) a homogeneous solid which undergoes no condensed phase reactions but regresses linearly, simply pyrolyzing from solid to vapor, and 3) a quasi-steady gas phase.

An experimental program was undertaken to investigate the validity of these assumptions to the extent possible. In an effort to study the regression of the surface and to study the reactions of the ingredients, cinephotomicrography was used. These motion pictures indicated that: 1) polyurethane binder was molten at the surface; 2) ammonium perchlorate particles are covered with a molten layer at the surface for both types of propellant; 3) at the pressure normally associated with nonacoustic instability the AP particles in the PU-AP propellant protruded above the binder and were then rapidly consumed, while CTPB propellants did not display this rapid consumption of the AP particles.

A scanning electron microscope was used to examine the details of quenched samples of PU-AP and CTPB-AP propellants.[15] The micrographs agreed with the preceding observations to the extent that the AP particles in the PU-AP propellant did protrude above the binder and were somewhat undercut, allowing three-dimensional energy transfer (Fig. 6).

From these observations the tenuous nature of the assumption that the propellant regresses as a one-dimensional, homogeneous solid is revealed. Although microscopically the surface regression is far from one dimensional, it is possible that the one-dimensional assumption can be used to approximate the macroscopic regression. Indeed, the major question may well be one of the heterogeneity of a propellant,

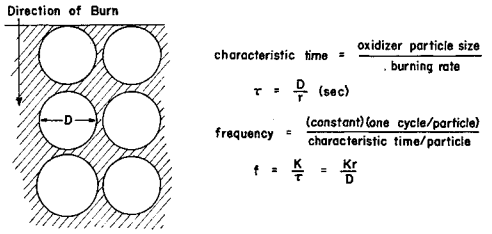

Fig. 7 The layer-frequency concept. The frequency at which a combustion wave burns through layered particles is directly proportional to the burning rate and inversely proportional to the diameter.

especially for PU propellants where, due to the undercutting observed in the SEM micrographs, the protruding AP particle is subjected to three-dimensional heating and is rapidly consumed.

In an effort to understand the effects of heterogeneity in polyurethane propellants undergoing nonacoustic instability, a computational scheme (the layer frequency concept of Refs. 10-11) was proposed. This computational scheme is based on an idealized propellant having oxidizer particles stacked one on top of another, surrounded by binder (Fig. 7).

A characteristic time for the surface variation is the time to burn through one particle, the particle diameter divided by the burning rate (i.e., $\tau = D/r$). If the particles are stacked in layers, this characteristic time will correspond to a frequency of one cycle per particle, or $f = 1/\tau = r/D$ (Fig. 7). Looking at an arrangement such as Fig. 8 (which is more typical of an actual propellant than is Fig. 7), one sees that the characteristic time is the time to repopulate the surface of the propellant with ammonium perchlorate particles. If enough AP particles at the surface undergo rapid consumption due to the undercutting and subsequent three-dimensional heating of the crystals (both the motion picture and the SEM micrographs show a large number of AP particles on the surface in about the same stage of consumption), and if the resulting minute pressure pulses were "in phase" with one another then measurable pressure fluctuations would occur. Thus, Fig. 8 represents a phase correlated‡ surface.

In an actual propellant, the oxidizer particles are randomly distributed, therefore, the phase correlation of the entire surface would be somewhat difficult to achieve and would most likely result in a frequency different from that noted previously. That is,

$$f = K/\tau = Kr/D$$

where K would be a measure of the randomness of the mix. For an idealized propellant like the one depicted in Fig. 8 one can arrive at the characteristic intersection diameter, D'

$$D' = (\tfrac{2}{3})^{1/2}D$$

where D = original particle diameter.[18]

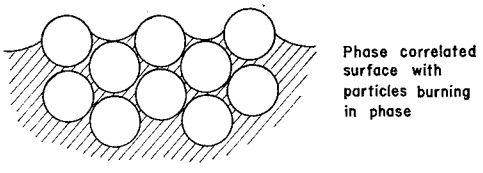

Fig. 8 Phase correlation. If the burning surface arranges itself such that sufficient oxidizer particles are exposed simultaneously, then the surface is said to be phase correlated, and measurable oscillations will occur at the layer frequency.

‡ This phase correlation concept was first proposed by Price[16] in connection with the accumulation and shedding of agglomerated metal from a propellant surface.

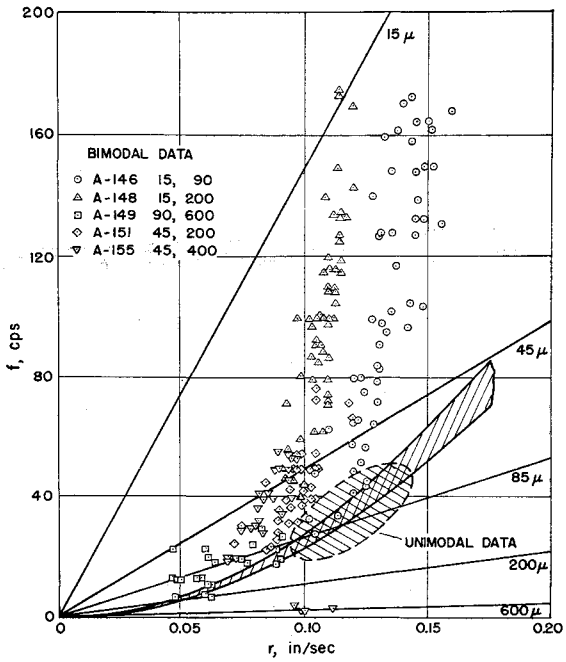

Fig. 9 Frequency vs burning rate for the polyurethane propellants tested. The predicted behavior (based on the one-dimensional models) is indicated by the cross-hatched parabolic band. The straight lines are the mapping of the equation $f = Kr/D$, with K = 0.83.

If $\delta \equiv$ average burning distance between particles (i.e., binder thickness) then the characteristic time τ' averaged over a long period of time or for a large number of particles would be given by $\tau' = (\delta + D')/r$ and the layer frequency would be

$$1/f = \tau' = \bar{r}/[\delta + (\tfrac{2}{3})^{1/2}D] = \bar{r}/\{D[\delta/D + (\tfrac{2}{3})^{1/2}]\}$$

so that $K = 1/[\delta/D + (\tfrac{2}{3})^{1/2}]$

It can be shown that for uniform-sized, spherical oxidizer crystals

$$\delta/D = \{\pi/6[1 + (\rho_{ox}/\rho_f)(1 - x/x)]^{1/3} - (\tfrac{2}{3})^{1/2}\}$$

and therefore,

$$K = \frac{1}{(6/\pi\{1 + (\rho_{ox}/\rho_f)[(1 - x)/x]\})^{1/3}}$$

where x = % oxidizer. For 75% unimodal AP + 25% PU (i.e., A-35) $K = 1.05$. A similar expression can be derived for bimodal propellants, giving

$$K_1 = \left\{\frac{x_1}{(6\pi)\ [x_T + (\rho_{ox}/\rho_f)(1 - x_T)]}\right\}^{1/3}$$

where x_1 = one of the bimodal fractions, x_T = total oxidizer loading; hence for 50/50 bimodal $K_1 = 0.83$, for 70/30 bimodal $K_1 = 0.93$, for 30/70 bimodal $K_1 = 0.70$.

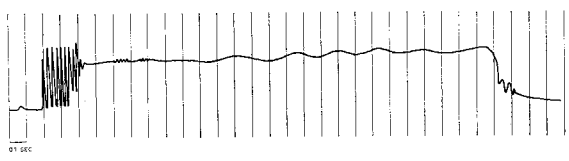

Fig. 10 Oscillograph trace for propellant A-155 shows dual frequency.

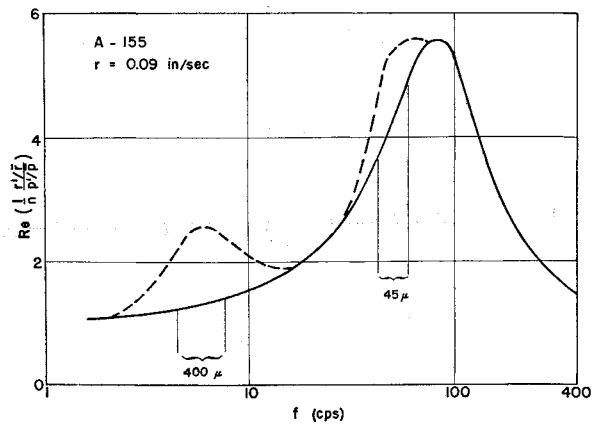

Fig. 11 Hypothesized response function with deviations included (the dashed lines) to account for oxidizer particle size.

The nonacoustic instability data for the polyurethane propellants are plotted as frequency vs burning rate in Fig. 9 (as suggested by the layer-frequency computational scheme). The straight lines represent the mapping of $f = Kr/D$ for the different particle sizes, and the data are for the various propellants (typically, pressures were 200 psi or less). The cross-hatched parabolic band represents the prediction of one-dimensional theory for the unimodal propellant A-35 with $A = 11$ and $B = 0.8$. The lower parabola represents the stability limit with the growth constant equal to zero. The upper bound reflects the most severe value of $\alpha\ \tau_{ch}$ determined for the A-35 propellant. Since the other polyurethane propellants were chemically identical to A-35, one might expect little change in the values of A and B parameters for the various propellants. Hence, one might also expect the data for the bimodal propellants to fall within the parabolic band, but this is not the case.

The one-dimensional theory parabola deviates significantly from the experimental results for the A-151 propellant (45- and 200-μ), as shown in Fig. 9. For a burning rate of 0.10 in./sec, the thermal wave thickness for the propellant is approximately 45 μ, which coincides with the fine oxidizer particle size for this propellant. Hence, deviations from one-dimensional behavior might be expected for this range of conditions.

Because of the similarity in the propellant compositions, the data for propellants A-146 and A-148 are quite similar, as might be expected. Both propellants contain 15-μ AP, and both oscillated at frequencies two to three times what normally would have been expected. A transition apparently occurred from one-dimensional behavior at low burning rates to a layer-frequency type of behavior at the higher burning rates.

Propellant A-155 not only exhibited the higher trend in frequencies, but under certain conditions, oscillated at very low frequencies; a single record would have two frequencies—a high frequency at the beginning of a run with a transition to a lower frequency. The low frequency corresponds very closely to the layer frequency of the large oxidizer particles. Apparently, a sufficient number of the large oxidizer particles were burning in phase with each other to cause an oscillation of sufficient magnitude to be measurable. Figure 10 is a pressure-time trace of one of the runs where the dual frequency oscillation occurred. The chuffing and oscillations that occurred at the initial part of the test were at a frequency of 52 cps, while the low-amplitude oscillations later in the test were at a frequency of 2.7 cps. This evidence indicates that the idea of phase correlation of oxidizer particles is apparently valid and can produce an observable effect under certain conditions. Other test records also exhibit this dual frequency.

Discussion of Response Functions

In the past, response function curves have been plotted in two dimensions; such as $Re\ R/n$ vs Ω. A more realistic approach is needed; one that accounts for behavior not included in the one-dimensional models. Therefore, a third axis might be added, and a three-dimensional contour, rather than a single two-dimensional curve, should be drawn. The response function curves normally considered (such as Figs. 1 and 2) become a cross-section of the contour.[13] In this study, it has been shown that f vs r may be used as such an indicator in the case of polyurethane propellants (due to the heterogeneity of these propellants). Therefore, ReR vs f vs r can be plotted, taking the form of a contour map. On the map there will possibly be three ridges (if the propellant is bimodal), two corresponding to the layer frequencies, and the third corresponding to the maximum in the one-dimensional theory. By taking a section of the contour at a constant burning rate (r = 0.09 in/sec), a modified form of the response function can be postulated as in Fig. 11. The dashed lines represent the approximate effect that might be caused by the layer frequency (it has been assumed that the two effects would be additive).

Conclusions and Implications for Future Work

The results of this study indicate that available models cannot adequately predict the nonacoustic instability behavior of composite propellants. This paper has also shown that models which assume the propellant to be a homogeneous solid do not predict the nonacoustic combustion instability of polyurethane propellants. For this class of propellants the "homogeneous solid" assumption is not valid when the thermal wave thickness is approximately equal to the oxidizer particle; the size of the oxidizer particles can then be a contributing (and possibly the dominating) factor of combustion instability. A simple mechanistic argument, such as the layer-frequency concept which accounts for and is able to predict the effect of oxidizer particle size on the frequency of oscillation, is not adequate to predict the other parameters of instability (such as magnitude of oscillations) since it is not based on any conservation laws. However, by combining aspects of existing models and computational schemes such as the layer-frequency concept, a greater understanding of the problem may possibly be obtained. Such understanding is not only essential but must be incorporated into mathematical models if those models are to predict combustion instability behavior.

References

[1] Akiba, R. and Tanno, M., "Low Frequency Instability in Solid Propellant Rocket Motors," *Proceedings of the First Symposium (International) on Rockets and Astronautics*, Tokyo, 1959, pp. 74–82.

[2] Sehgal, R. and Strand, L., "A Theory of Low-Frequency Combustion Instability in Solid Rocket Motors," *AIAA Journal*, Vol. 2, No. 4, April 1964, pp. 696–702.

[3] Beckstead, M. W., Ryan, N. W., and Baer, A. D., "Nonacoustic Instability of Composite Propellant Combustion," *AIAA Journal*, Vol. 4, No. 9, Sept. 1966, pp. 1622–1628.

[4] Coates, R. L., Cohen, N. S., and Harvill, L. R., "An Interpretation of L^* Combustion Instability in Terms of Acoustic Instability Theory," *AIAA Journal*, Vol. 5, No. 6, June 1967, pp. 1097–1102.

[5] Beckstead, M. W. and Price, E. W., "Nonacoustic Combustor Instability," *AIAA Journal*, Vol. 5, No. 11, Nov. 1967, pp. 1989–1996.

[6] Oberg, C. L., "Combustion Instability: The Relationship between Acoustic and Nonacoustic Instability," *AIAA Journal*, Vol. 6, No. 2, Feb. 1968, pp. 265–270.

[7] "Combustion of Solid Propellants and Low Frequency Combustion Instability," Technical Publication NOTS TP 4244, June 1967, Aerothermochemistry Division, U.S. Naval Ordnance Test Station, China Lake, Calif.

[8] Beckstead, M. W., "Low Frequency Instability: A Comparison of Theory and Experiment," *Combustion and Flame*, Vol. 12, Oct. 1968, pp. 417–426.

[9] Beckstead, M. W. and Culick, F. E. C., "A Comparison of Analysis and Experiment for Solid Propellant Combustion Instability," Technical Publication NWC TP 4531, May 1968, Naval Weapons Center, China Lake, Calif.

[10] "Combustion of Solid Propellants and Low Frequency Combustion Instability," Technical Publ. NWC TP 4478 April 1968, Aerothermochemistry Div., Naval Weapons Center, China Lake, Calif.

[11] Beckstead, M. W. and Boggs, T. L., "The Effect of Oxidizer Particle Size on Nonacoustic Instability," Fourth ICRPG Combustion Conference, Stanford Research Institute, Menlo Park, Calif., Oct. 1967.

[12] Mathes, H. B., Boggs, T. L., Dehority, G. L., and Crump, J. E., "Low Frequency Combustion Instability Progress Report," Technical Publication NWC TP 4565, Dec. 1968, Naval Weapons Center, China Lake, Calif.

[13] Beckstead, M. W., Mathes, H. B., Price, E. W., and Culick, F. E. C., "Combustion Instability of Solid Propellants," *12th Combustion (International) Symposium*, The Combustion Institute, 1969, pp. 203–211.

[14] Culick, F. E. C., "A Review of Calculations for Unsteady Burning of a Solid Propellant," *AIAA Journal*, Vol. 6, No. 12, Dec. 1968, pp. 2241–2255.

[15] Boggs, T. L., Prentice, J. L., Kraeutle, K. J., and Crump, J. E., "The Role of the Scanning Electron Microscope in the Study of Solid Propellant Combustion," *Proceedings of the Second Annual Scanning Electron Microscope Symposium*, Chicago, April 1969, pp. 349–364.

[16] Price, E. W., "Review of the Combustion Instability Characteristics of Solid Propellants," *Advances in Tactical Rocket Propulsion, AGARD Conference Proceedings No. 1*, April 1965, edited by S. S. Penner, Maidenhead, England, Technivision Services, Aug. 1968, pp. 141–194.

[17] Blum, E. H. and Wilhelm, R. H., "A Statistical Geometric Approach to Random-Packed Beds," *AIChE International Chemical Engineering Symposium Series*, No. 4, 1965, London, pp. 21–27.